Room-temperature phosphorescence from bamboo fibers and designed materials

Yingxiang Zhai[1,2,+], *Jingyi Zhou*[1,2,+], *Ben Dang*[1,2,+], *Xinping Cui*[1,2], *Shouxin Liu*[1], *Xuetong Shi*[3], *Ran Bi*[3], *Jian Li*[1], *Shujun Li**[,1,2], *Orlando J. Rojas**[,3] and *Zhijun Chen**[,1,2]

[1] Key Laboratory of Bio-based Material Science and Technology of Ministry of Education, Northeast Forestry University, Harbin 150040, P.R. China. E-mail: chenzhijun@nefu.edu.cn; lishujun@nefu.edu.cn

[2] Heilongjiang International Joint Lab of Advanced Biomass Materials, Northeast Forestry University, Harbin 150040, P.R. China. E-mail: chenzhijun@nefu.edu.cn; lishujun@nefu.edu.cn

[3] Bioproducts Institute, Department of Chemical and Biological Engineering, University of British Columbia, 2360 East Mall, Vancouver, BC V6T 1Z3, Canada. E-mail: orlando.rojas@ubc.ca

[4] Department of Chemistry, 2036 Main Mall. Vancouver, The University of British Columbia, Vancouver, BC Canada V6T 1Z1.

[5] Department of Wood Science, The University of British Columbia, 2900-2424 Main Mall Vancouver, BC Canada V6T 1Z4.

[+] These authors contributed equally to this work.

[*] Corresponding authors Emails: chenzhijun@nefu.edu.cn (S. Li.); lishujun@nefu.edu.cn (Z. Chen); orlando.rojas@ubc.ca (O. J. Rojas),

SUMMARY

Recent developments in room-temperature phosphorescence (RTP) from biobased polymers have shown great promise in realizing sustainable RTP systems. Here, we introduce an efficient "top-down" method to achieve RTP biofibers using sixteen species of bamboo following partial delignification (B-fibers). The photophysical characterization combined with structural, surface and chemical inquiries (XRD, XPS, FTIR) along with DFT calculations revealed the fundamental reasons for RTP, associated with the interactions between cellulose, hemicelluloses and the residual lignin. Multiple emissive oxygen-containing clusters and aromatic chromophores in the B-fibers were shown to be RTP-active (wavelengths going from 450 to 530 nm at an increased excitation from 240 to 360 nm). Green afterglow with a lifetime of 294.9 ms (excitation wavelength = 270 nm) was observed while blue fluorescence and long-lived yellow-green RTP took place under 365 nm irradiation. Such effects were modulated by the crystalline environment and hydrogen bonding interactions. The RTP emission of the B-fibers was found to be sensitive to temperature, excitation and humidity. Moreover, when combined with a water-soluble fluorescent dye (following simple immersion), red afterglow emission was demonstrated under the effect of energy-transfer. Following these results, we synthesized functional luminescent materials (paper, films, textiles and aerogels), proposed herein as practical, sustainable and compostable choices for photoexcitation in the visible range.

1. INTRODUCTION

Organic room-temperature phosphorescence (RTP) is most relevant to a wide range of applications, including bioimaging[1,2], anticounterfeiting[3,4], organic light-emitting diode[5,6], X-ray scintillator[7,8] and information storage technologies[9,10]. The key attributes of such systems is flexible structural design and tunable optical performance. Generally, two main principles are operative in organic RTP materials[9,11-14]. The first involves intersystem crossing (ISC) by singlet excitons conversion to triplet excitons. As the dominant driving force of ISC, strong and efficient spin-orbit coupling (SOC) can be realized by introducing aromatic carbonyl groups, deuterated carbon atoms, halogens, and heteroatoms with lone-pair electrons. (The second principle relates to radiative migration of triplet excitons to the ground state, which is usually achieved by rigidifying the chromophores *via* crystallization, polymerization and matrix solidification.

Guided by the above-mentioned principles, several organic RTP materials, such as molecular crystals[15], supramolecules[16], polymer composites[17], COF[18] and MOF[19] have been developed.

These materials can be processed into RTP powders, films, liquids, structural materials and fibers[20,21]. The latter have shown great potential and bottom-up approaches have been explored for their production *via* doping synthesized phosphors into polymeric fibers[22]. For example, organic phosphors[23], perovskites[24], transition elements[25] and sulfide materials[26] can be doped in a polymer matrix to achieve photoluminescence in the respective optical fibers. However, these technologies suffer from costly and complex processing and mostly rely on resources based on fossil carbon.

Recently, RTP materials from biomass have captured interest given their favorable sustainability metrics, abundance and cost-effectiveness as well as end of life considerations (biodegradability, compostability)[3,27]. Until now, wood[28-30], lignin[31-34], gelatin[35], hemicellulose[36], cellulose[20,37,38] and natural polyphenols[39] have been successfully used as precursors of RTP materials. Less attention has been paid to whole plant structures containing some of the latter biomacromolecules. For instance, bamboo is an appealing option given its abundance, fast growth rate, strength, structure and composition. However, RTP materials from bamboo are still an incipient area of research, which is the subject of the current investigation related to the "top-down" synthesis of RTP fibers (**Fig. 1**)[40,41]. Specifically, hemicellulose and lignin were partially removed from bamboo, yielding microfibers that showed room-temperature phosphorescence.

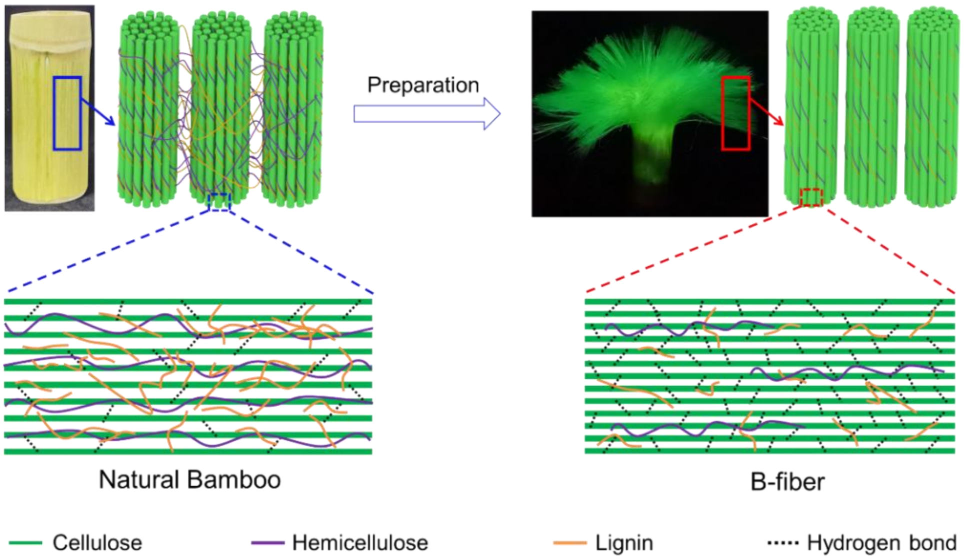

Fig. 1. Schematic illustration showing the top-down development of RTP fibers from natural bamboo.

2. RESULTS

2.1 B-fibers with RTP emission. The UV-Vis spectra of bamboo exhibit a main absorbance between 250 and 400 nm (**Supplementary Fig. 1**). Moreover, upon excitation, bamboo shows fluorescence at 435 nm (**Fig. 2a**) and long-lasting RTP emission at 480 nm, with lifetime of 90.4 ms (**Fig. 2b** and **2c)**. These observations prompted our present inquiries to explore bamboo-based RTP fibers. Treatment with peroxyacetic acid (**Fig. 2d-2e** and **Supplementary Fig. 2**) was effective in partially removing hemicelluloses and lignin, unraveling the "**B-fibers**", which were analyzed by comparing their NMR spectra with that of natural bamboo (**Supplementary Fig. 3**). The cellulose, hemicellulose and lignin content in B-fibers were determined to be 85.8%, 6.1% and 1.1%, respectively (these components amounted to 58.3%, 14.5% and 23.8% in the unmodified bamboo). The **B-fibers** showed a high mechanical strength (tensile strengthen and Young's modulus of *ca*. 424 MPa and 22 GPa, respectively), making them stronger than cotton and silk fibers (**Supplementary Fig. 4**). The B-fiber system exhibited RTP emission (**Fig. 2f**), with a lifetime of 294.9 ms (excitation wavelength = 270 nm), surpassing the original bamboo (**Supplementary Fig. 5**). To test whether the proposed strategy can be expanded to other bamboo species, B-fibers were obtained from other sources. As such, we found that the RTP lifetimes ranged from *ca.* 160 to 347 ms, depending on the species (**Fig. 2g**). Moreover, blue fluorescence and long-lived yellow-green RTP were observed when irradiated at 365 nm (**Supplementary Fig. 6**).

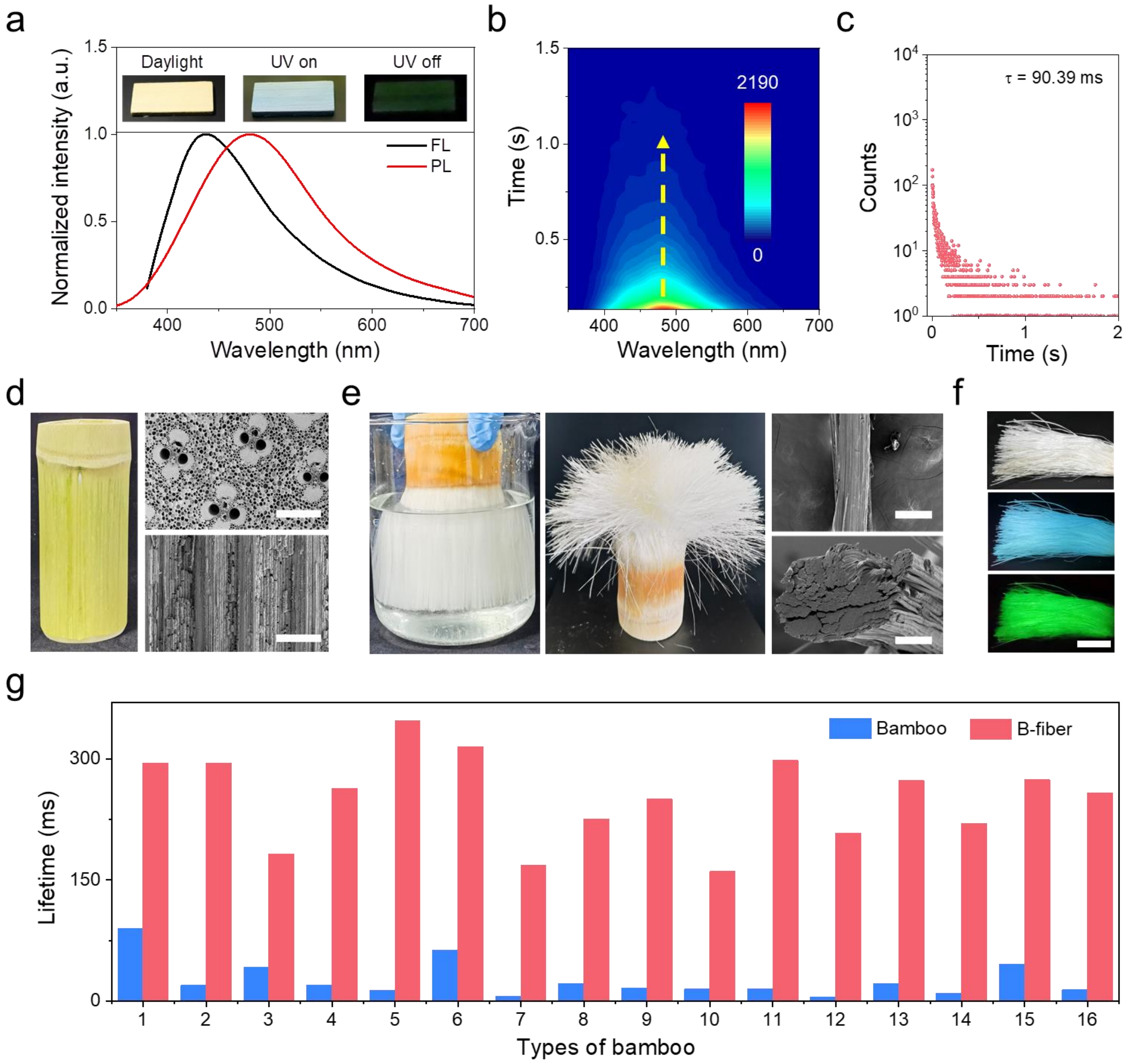

Fig. 2. **RTP properties of bamboo and B-fibers**. *Natural bamboo*: (a) Fluorescence and RTP spectra, (b) time-dependent RTP spectra and (c) RTP lifetime decay. (d) Digital images (left) and SEM images of natural bamboo (top-down view, upper; cross-section view, bottom) (right). The scale bar corresponds to 500 nm. *B-fibers:* (e) Digital images of B-fibers in water (left), dried B-fibers (middle) and SEM images of B-fibers (right). Scale bar = 100 nm. (f) Digital images of B-fibers in day light (upper), upon UV irradiation (middle) and after removing UV excitation (down), scale bar = 2 cm. (g) RTP lifetime of B-fibers made from different types of bamboo species (1, *Phyllostachys edulis* (Carrière) J. Houz.; 2, *Phyllostachys reticulata* (Rupr.) K. Koch; 3, *Pseudosasa amabilis* (McClure) P. C. Keng ex S. L. Chen & al.; 4, *Bambusa rutile* McClure; 5, *Pleioblastus maculatus* (McClure) C. D. Chu & C. S. Chao; 6, Oligostachyum sulcatum; 7, *Bambusa multiplex* (Lour.) Raeusch. ex Schult. & Schult. f.; 8, *Phyllostachys vivax* McClure; 9, *Indosasa gigantea* (T. H. Wen) T. H. Wen; 10, *Phyllostachys parvifolia* C. D. Chu & H. Y. Chou; 11, *Sinobambusa tootsik* (Makino) Makino; 12, *Phyllostachys violascens 'Prevernalis'* S.Y.Chen et C.Y.Yao; 13, *Phyllostachys heteroclada* Oliv.; 14, Phyllostachys aureosulcata ‘Aureocaulis’; 15, *Phyllostachys sulphurea var. viridis* R. A. Young; 16, *Phyllostachys prominens* W. Y. Xiong.). The measurement conditions for the RTP spectra and lifetime corresponded to 10 ms delay, room temperature, excitation wavelength = 270 nm.

2.2 Tunable RTP emission. The RTP intensity and lifetime of B-fibers (*Phyllostachys edulis* (Carrière) J. Houz) were demonstrated for their tunability (**Fig. 3a** and **Supplementary Fig. 7**). Particularly, the RTP lifetime decreased from 757.3 ms to 39.2 ms when the temperature increased from 77 K to 400 K. Such temperature-dependent RTP emission is explained by non-radiative migration of triplet excitons promoted at high temperatures. Additionally, the B-fibers exhibited quenched RTP emission when exposed to humid environments (**Supplementary Fig. 8**). Specifically, the RTP lifetime decreased from 294.9 ms to 19.8 ms when the humidity increased from 0% to 90%. Interestingly, the lifetime was recovered by drying the wet B-fibers. Though some losses were noted after "humidity-drying" cycles, the optical robustness of the fibers was largely maintained (**Fig. 3b**).

The RTP emission of the B-fibers was sensitive to the excitation wavelength: the RTP wavelength changed from 450 nm to 530 nm when the excitation wavelength increased from 240 nm to 360 nm (**Fig. 3c**). More interestingly, RTP emission of the B-fibers overlapped with rhodamine B (RhB) absorbance, suggesting the possibility of energy transfer between B-fiber and RhB (**Supplementary Fig. 9**). To test this hypothesis, we immersed the B-fibers in RhB solution and the as-obtained B-fiber/RhB system exhibited red afterglow emission upon UV excitation, matching the fluorescence spectra of RhB (**Fig. 3d**). The lifetime of red afterglow emission from RhB in the B-fiber/RhB was 73.59 ms (**Supplementary Fig. 10**).

To investigate the energy transfer process between the B-fiber and RhB, the photophysical properties of the donor (B-fiber) and acceptor (RhB) were measured. With an increased concentration of RhB (0 to 200 μg/mL), the emission spectra of the B-fiber/RhB system (λ_{ex} = 270 nm) exhibited a gradual reduction of phosphorescence emission, centered at 490 nm. Meanwhile, a concomitant enhancement of RhB fluorescence took place in the 580-700 nm region, which indicates an efficient energy transfer from the triplet state of the donor to the acceptor molecules (**Supplementary Fig. 11**). The highest energy transfer efficiency reached 80.2% at 200 μg/mL RhB (**Supplementary Fig. 12**). The time-resolved emission of the B-fibers with increased RhB content was monitored at 490 nm (λ_{ex} = 270 nm): a gradual lifetime reduction was observed going from 294.03 ms to 112.78 ms (**Supplementary Fig. 13**).

Efficient non-radiative FRET from the triplet state of the B-fiber donor to the singlet states of the RhB acceptor (TS-FRET) was confirmed by the decay profiles thereby eliminating the possibility of simple energy transfer (emission-reabsorption process), since for this situation the donor lifetime was not expected to change. On the other hand, no afterglow emission in B-fiber/RhB was observed upon excitation of the RhB acceptor at 500 nm (**Supplementary Fig. 14**). Taken the results together, it is evident that the long-lived triplet excitons of the donor B-fiber were the only source of the delayed population of the singlet state of the acceptor RhB *via* an efficient TS-FRET mechanism, resulting in persistent delayed fluorescence.

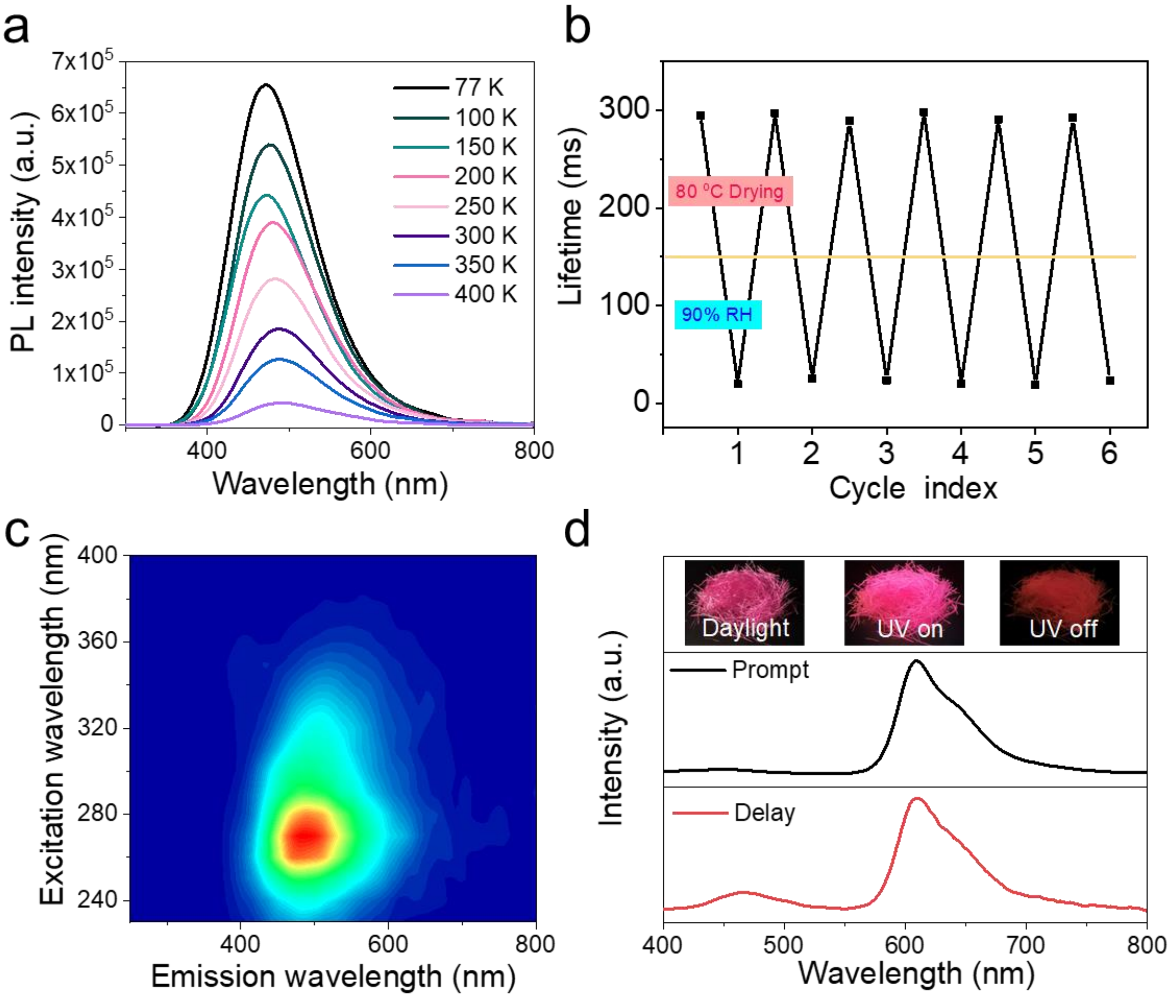

Fig. 3. **Tunable RTP properties of B-fiber.** (a) RTP spectra of B-fibers at different temperature. (b) RTP lifetimes of B-fibers after "drying-humidity" cycles. (c) RTP emissions of B-fibers using different excitation wavelengths. (d) Fluorescence and phosphorescence spectra of B-fibers/RhB. The measurement conditions for the RTP spectra and lifetime included 10 ms delay, room temperature, excitation wavelength = 270 nm.

2.3 Mechanistic interpretation of RTP from B-fibers. To understand the interaction between the components, DFT calculations were performed assuming polysaccharide chains and single aromatic ring as model structures for cellulose/hemicellulose and lignin. The simulation results showed that polysaccharides tended to form strong hydrogen bonds (**Fig. 4a**). They also interacted with lignin *via* hydrogen bonding and van der Waals interactions (**Fig. 4a**). These results indicate that lignin was confined by the cellulose/hemicellulose in bamboo and B-fibers. Also, hydroxyl moieties of cellulose/hemicellulose formed molecular clusters. Molecular confinement and clusters promoted radiative migration of triplet excitons and RTP emission. Such multiple emissive centers were confirmed by the excitation-dependent RTP emission, as demonstrated previously (**Fig. 3c**)

As expected, the relative concentrations of cellulose, hemicellulose and lignin in the B-fibers were different from those of the precursor bamboo. Such components contributed to the different RTP behavior. XPS analysis showed that the C-O ratio was higher and oxygen-incorporated moieties increased by converting bamboo into B-fibers, given the oxidative process (**Supplementary Fig. 15**)[42,43]. Additionally, B-fibers presented C-O, C=O and O-C-O structures, less evident in the natural bamboo. Such moieties tend to form emissive clusters and enhanced spin-orbit coupling (SOC), favoring RTP emission (**Fig. 4b**). FT-IR also confirmed these observations: the intensity of hydroxyl signals in B-fibers was stronger than in natural bamboo. Moreover, the FT-IR signals of hydroxyl moieties in B-fibers shifted to 3360 cm^{-1} while the signal of bamboo was at 3413 cm^{-1}, suggesting that a stronger hydrogen bonding take place in B-fibers compared to natural bamboo[44,45], stabilizing the triplet excitons and preventing the diffusion of oxygen and humidity (**Fig. 4c**). Additionally, XRD spectra suggested that B-fibers formed more crystallized cellulose structures compared to natural bamboo, providing a better environment for RTP emission (**Fig. 4d**). Overall, the increased oxygen-incorporated moieties, hydrogen bonding and crystallinity cooperatively contributed to the enhanced RTP of the B-fibers.

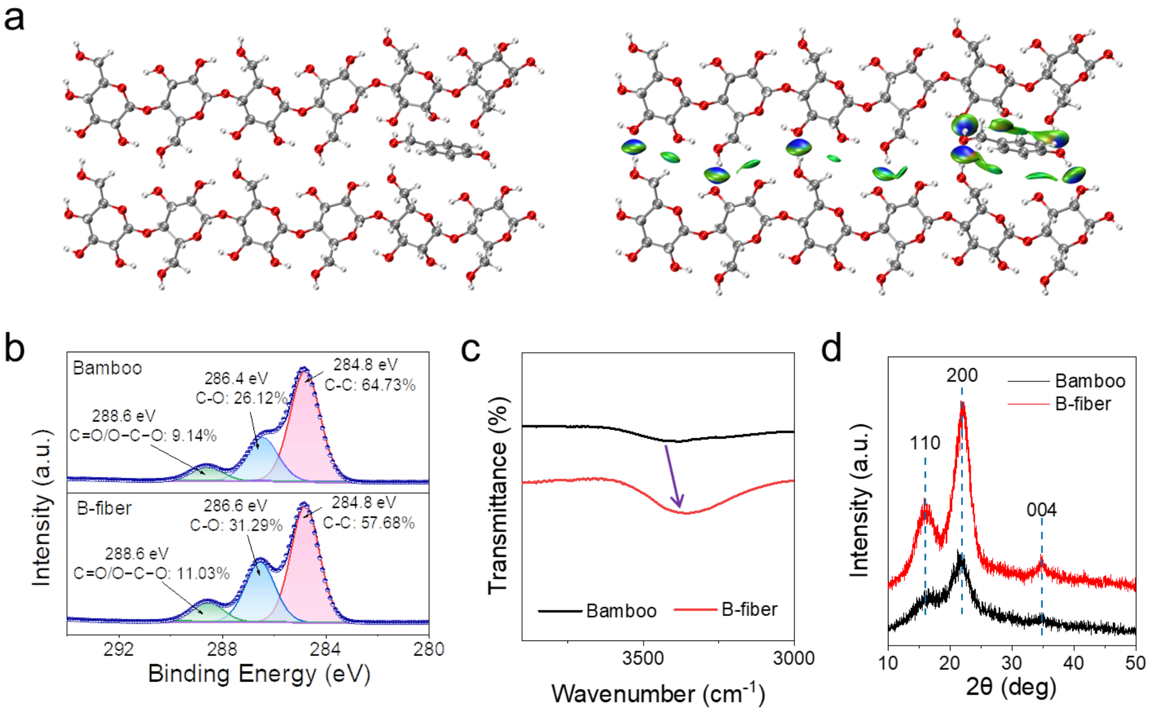

Fig. 4. **Mechanistic investigation.** (a) Results from calculated interactions between polysaccharides and lignin (DFT): Confirmation (left) and independent gradient model (right). (b) High resolution XPS C1S spectra of natural bamboo and B-fibers. (c) FT-IR spectra of natural bamboo and B-fibers. (d) XRD spectra of natural bamboo and B-fibers.

2.4 RTP demonstrators based on B-fibers. B-fibers and the original bamboo were used to build a variety of designed RTP materials (**Fig. 5a**). The designs based on B-fibers exhibited green afterglow emission after removing UV excitation (**Fig. 5a** and **Supplementary Video 1**). The afterglow color of the materials was conveniently tuned to red by pre-treatment with RhB *via* the TS-FRET process (**Fig. 5b**). Given the facile assembly, the B-fibers or B-fibers/RhB were incorporated in low-cost demonstration prototypes in given large scales (**Fig. 5c**). They included luminescent textiles (promising emissive materials for electronic displays and smart sensors) (**Fig. 5d**). In addition, B-fibers were used to prepare anti-counterfeit embroidery textiles (afterglow emission was observed from the given features after removing the UV irradiation, **Fig. 5e**). In order to demonstrate the applicability of the system, an afterglow paper sheet was prepared with B-fibers. The paper sheet was flexible and exhibited afterglow emission after UV irradiation (**Fig. 5f** and **5g**). The afterglow was investigated for anti-counterfeiting applications, e.g., by printing with a commercial printer. Importantly, the afterglow emission remained after paper printing (**Fig. 5h**). As a control, no afterglow emission was observed for normal printed paper (**Supplementary Fig. 16**). Encrypted documents were created by taking advantage of the TS-FRET between B-fiber and RhB (**Fig. 5i** and **Fig. 5j**). In this way, on UV irradiation, the paper displayed a red afterglow pattern and given pre-designed images were observed after switching off the UV light (**Fig. 5i** and **Fig. 5j**). As control, no afterglow emission was observed when printing RhB on commercially available paper (**Supplementary Fig. 17** and **Supplementary Fig. 18**). Finally, B-fibers were physically blended with polyvinyl alcohol (PVA) to prepare transparent and flexible RTP films with afterglow emission (**Fig. 5k**) and as also building blocks for producing RTP foams with afterglow emission (**Fig. 5l**). Overall, the results confirmed afterglow and significant potential for materials incorporating B-fibers in typical processing methods.

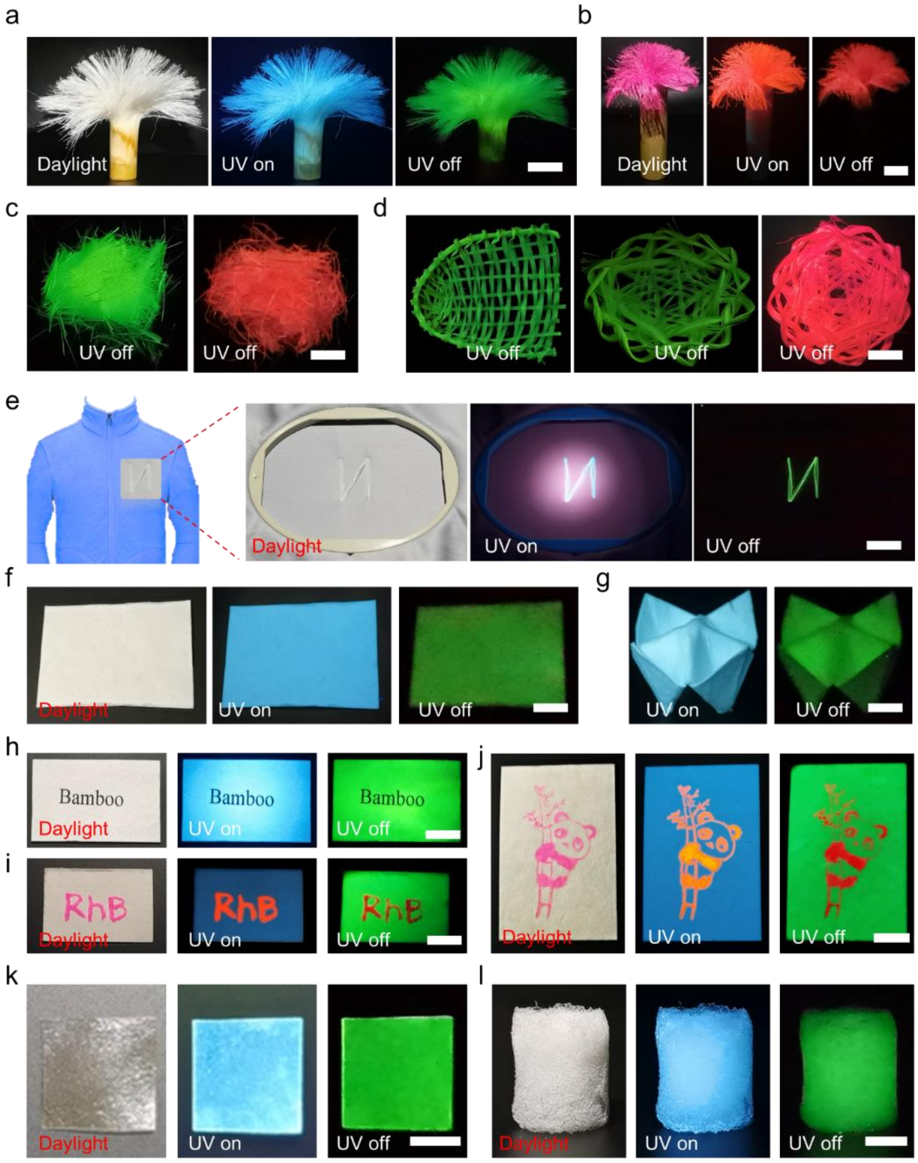

Fig. 5. **Applications.** Material prototypes based on B-fibers before (on) and after (off) UV irradiation: (a) Bamboo with B-fibers, scale bar = 4 cm. (b) Bamboo with B-fibers/RhB, bamboo with B-fibers/RhB, scale bar = 3 cm. (c) B-fibers and B-fibers/RhB, scale bar = 1 cm. (d) Textiles made from B-fibers and B-fibers/RhB, scale bar = 1 cm. (e) Embroidery made from B-fibers, scale bar = 1 cm. (f) Paper made from B-fibers, scale bar = 1 cm. (g) Folded paper made from B-fibers, scale bar = 1 cm. (h) Printed paper made from B-fibers, scale bar = 1 cm. (i) Paper made from B-fibers with “RhB” printed using RhB, scale bar = 1 cm. (j) Paper made from B-fibers with a RhB-printed image, scale bar = 1 cm. (k) PVA/B-fibers film, scale bar = 0.5 cm. (l) B-fibers-based solid foam, scale bar = 1 cm.

3. DISCUSSION

In summary, RTP fibers (B-fibers) were produced from natural bamboo by partial delignification. Attributed to the interactions between cellulose, hemicelluloses and lignin, the as-obtained B-fibers exhibited long-lived RTP emission (lifetime of 294.9 ms). Moreover, B-fibers with red afterglow emission were obtained by simply treatment with RhB *via* an energy transfer process. The B-fibers and B-fibers/RhB were easily processed into multifunctional RTP materials. Different from the traditional “bottom-up” methods used to produce RTP materials, which are costly and have negative environmentally impacts, the as-developed “top-down” RTP B-fibers can be easily produced from bamboo. Our results provide a practical route for producing sustainable RTP fibers at low cost and on a large scale.

4. METHODS

4.1 Preparation of B-fibers

Raw bamboo culms were cut into individual stems of different lengths (without nodes) and boiled in water for 1 h to remove water-soluble organic matter and trapped air. Following, a delignifying solution (50 wt% glacial acetic acid and 50 wt% 30% H_2O_2) was applied by soaked soaking at 80 °C until the sample became light in color. The sample was then rinsed with 0.5 wt% sodium hydroxide aqueous solution for 5-10 min and washed in deionized water to remove any residual chemicals. Finally, the samples were placed in absolute ethanol for further washing and the obtained B-fibers was were dried at 60 ℃ for 24 h.

4.2 Preparation of B-fibers/RhB

A certain amount of RhB was weighed and dissolved in water to prepare aqueous solutions of

RhB of different concentrations. B-fibers were directly immersed in the given RhB aqueous solutions for 12 h at room temperature. The obtained samples were dried at 60 ℃ for 12 h to give B-fibers/RhB.

4.3 Preparation of RTP paper

Three (3) grams of B-fibers (on dry-weight basis) were fiberized using a laboratory disintegrator, yielding a B-fibers suspension that was directly used to prepare paper-sheets using a ZQJ1-B-II sheet former (China). The formed wet-sheets were pressed at 800 kPa for 5 min and dried at 105 °C for 10 min (5 min each side) to obtain RTP paper.

4.4 Preparation of PVA/B-fibers films

30 mg of B-fibers were added to 20 mL of a PVA aqueous solution (50 mg/mL). The as-obtained mixture was cast into membranes and dried at 60 °C for 4 h to obtain PVA/B-fibers film.

4.5 Preparation of B-fibers foams

B-fibers (50 mg) and deionized water (5 mL) were combined in 10-mL bottles. The mixture was then freeze-dried to give the given foams based on the B-fibers.

Acknowledgements

Z.J.C wishes to thank the National Natural Science Foundation of China (31890774). O.J.R., R.B and X.S, acknowledge funding support from the Canada Excellence Research Chair Program (CERC-2018-00006), Canada Foundation for Innovation (Project 38623) and Pacific Economic Development Canada (PacifiCAN).

Data Availability

All relevant data are included in this article and its Supplementary Information files.

Competing interests

The authors declare no competing interests.

References

1. Zhao, W., He, Z. & Tang, B. Z. Room-temperature phosphorescence from organic aggregates. *Nat. Rev. Mater.* **5,** 869-885 (2020).
2. Dang, Q., et al. Room-temperature phosphorescence resonance energy transfer for construction of near-infrared afterglow imaging agents. *Adv. Mater.* **32,** 2006752 (2020).

3. Luo, X., et al. Room-temperature phosphorescent materials derived from natural resources. *Nat. Rev. Chem.* **7,** 800-812 (2023).
4. Shi, L., Ding, L., Zhang, Y. & Lu, S. Application of room-temperature phosphorescent carbon dots in information encryption and anti-counterfeiting. *Nano Today* **55,** 102200 (2024).
5. Zhang, Y., et al. Large-area, flexible, transparent, and long-lived polymer-based phosphorescence films. *J. Am. Chem. Soc.* **143,** 13675-13685 (2021).
6. Ma, W., Bin, Z., Yang, G., Liu, J. & You, J. Structurally nontraditional bipolar hosts for RGB phosphorescent OLEDs: boosted by a "butterfly-shaped" medium-ring acceptor. *Angew. Chem. Int. Edit.* **61,** e202116681 (2022).
7. Gan, N., et al. Organic phosphorescent scintillation from copolymers by X-ray irradiation. *Nat. Commun.* **13,** 3995 (2022).
8. Dong, M., et al. Polymorphism-dependent organic room temperature phosphorescent scintillation for X-ray imaging. *Adv. Mater.* 2310663 (2024).
9. Dai, X.-Y., Huo, M. & Liu, Y. Phosphorescence resonance energy transfer from purely organic supramolecular assembly. *Nat. Rev. Chem.* **7,** 854-874 (2023).
10. Wu, Z., Bergmann, K. & Hudson, Z. M. Dopants induce persistent room temperature phosphorescence in triarylamine boronate esters. *Angew. Chem. Int. Edit.* **63,** e202319089 (2024).
11. Yang, X., Waterhouse, G. I. N., Lu, S. & Yu, J. Recent advances in the design of afterglow materials: mechanisms, structural regulation strategies and applications. *Chem. Soc. Rev.* **52,** 8005-8058 (2023).
12. Guo, J., Yang, C. & Zhao, Y. Long-lived organic room-temperature phosphorescence from amorphous polymer systems. *Acc. Chem. Res.* **55,** 1160-1170 (2022).
13. Wang, H., et al. Abnormal thermally-stimulated dynamic organic phosphorescence. *Nat. Commun.* **15,** 2134 (2024).
14. Zhou, L., et al. Achieving efficient dark blue room-temperature phosphorescence with ultra-wide range tunable-lifetime. *Angew. Chem. Int. Edit.* e202403773 (2024).
15. Gu, L., et al. Colour-tunable ultra-long organic phosphorescence of a single-component molecular crystal. *Nat. Photonics.* **13,** 406-411 (2019).
16. Ma, X.-K. & Liu, Y. Supramolecular purely organic room-temperature phosphorescence. *Acc. Chem. Res.* **54,** 3403-3414 (2021).
17. Cheng, A., et al. Disorder-enhanced charge-transfer-mediated room-temperature phosphorescence in polymer media. *Angew. Chem. Int. Edit.* **62,** e202312627 (2023).
18. Hamzehpoor, E., et al. Efficient room-temperature phosphorescence of covalent organic frameworks through covalent halogen doping. *Nat. Chem.* **15,** 83-90 (2023).
19. Liu, H., et al. Highly efficient blue phosphorescence from pillar-layer MOFs by ligand functionalization. *Adv. Mater.* **34,** 2107612 (2022).
20. Zhang, X., et al. Ultralong phosphorescence cellulose with excellent anti-bacterial, water-resistant and ease-to-process performance. *Nat. Commun.* **13,** 1117 (2022).
21. Zhang, T., et al. Molecular engineering for metal-free amorphous materials with room-temperature phosphorescence. *Angew. Chem. Int. Edit.* **59,** 11206-11216 (2020).
22. Wang, Z., Shi, X. & Peng, H. Alternating current electroluminescent fibers for textile displays. *Natl. Sci. Rev.* **10,** nwac113 (2023).

23. Hwang, Y. H., et al. Bright-multicolor, highly efficient, and addressable phosphorescent organic light-emitting fibers: toward wearable textile information displays. *Adv. Funct. Mater.* **31,** 2009336 (2021).
24. Zhou, Y., et al. Single-crystal organometallic perovskite optical fibers. *Sci. Adv.* **8,** eabq8629 (2022).
25. Zhang, Z., et al. A colour-tunable, weavable fibre-shaped polymer light-emitting electrochemical cell. *Nat. Photonics.* **9,** 233-238 (2015).
26. Yang, C., et al. Ionotronic luminescent fibers, fabrics, and other configurations. *Adv. Mater.* **32,** 2005545 (2020).
27. Shi, X., Bi, R., Wan, Z., Jiang, F. & Rojas, O. J. Solid wood modification toward anisotropic elastic and insulative foam-like materials. *ACS Nano* **18,** 7959-7971 (2024).
28. Yuan, J., et al. Sustainable afterglow materials from lignin inspired by wood phosphorescence. *Cell Rep. Phys. Sci.* **2,** 100542 (2021).
29. Zhai, Y., et al. Room temperature phosphorescence from natural wood activated by external chloride anion treatment. *Nat. Commun.* **14,** 2614 (2023).
30. Liu, R., et al. Producing a room temperature phosphorescent film from natural wood using a top-down approach. *Adv. Funct. Mater.* **34,** 2312254 (2024).
31. Yang, M., et al. Repurposing lignin to generate functional afterglow paper. *Cell Rep. Phys. Sci.* **3,** 100867 (2022).
32. Wan, K., et al. Structural materials with afterglow room temperature phosphorescence activated by lignin oxidation. *Nat. Commun.* **13,** 5508 (2022).
33. Liu, R., Jiang, T., Liu, D. & Ma, X. A facile and green strategy to obtain organic room-temperature phosphorescence from natural lignin. *Sci. China Chem.* **65,** 1100-1104 (2022).
34. Guo, H., et al. Photocured room temperature phosphorescent materials from lignosulfonate. *Nat. Commun.* **15,** 1590 (2024).
35. Cai, S., et al. Ultralong organic phosphorescent foams with high mechanical strength. *J. Am. Chem. Soc.* **143,** 16256-16263 (2021).
36. Lu, B., et al. Natural ultralong hemicelluloses phosphorescence. *Cell Rep. Phys. Sci.* **3,** 101015 (2022).
37. Cao, M., et al. Biobased and biodegradable films exhibiting circularly polarized room temperature phosphorescence. *Nat. Commun.* **15,** 2375 (2024).
38. Peng, F., et al. Color-tunable, excitation-dependent, and water stimulus-responsive room-temperature phosphorescence cellulose for versatile applications. *Adv. Mater.* **35,** 2304032 (2023).
39. Wan, K., et al. Sustainable afterglow room-temperature phosphorescence emission materials generated using natural phenolics. *Angew. Chem. Int. Edit.* **61,** e202202760 (2022).
40. Li, Z., et al. Sustainable high-strength macrofibres extracted from natural bamboo. *Nat. Sustain.* **5,** 235-244 (2022).
41. Wang, J., et al. Green, sustainable architectural bamboo with high light transmission and excellent electromagnetic shielding as a candidate for energy-saving buildings. *Nano-Micro Lett.* **15,** 11 (2023).
42. Hoeger, I. C., et al. Bicomponent lignocellulose thin films to study the role of surface lignin in cellulolytic reactions. *Biomacromolecules* **13,** 3228-3240 (2012).

43. Zhu, L., et al. Transparent bioplastics from super-low lignin wood with abundant hydrophobic cellulose crystals. *ACS Sustain. Chem. Eng.* **10,** 13775-13785 (2022).

44. Guo, Y. & Wu, P. Investigation of the hydrogen-bond structure of cellulose diacetate by two-dimensional infrared correlation spectroscopy. *Carbohyd. Polym.* **74,** 509-513 (2008).

45. Chen, S., et al. Hydrogen-bonded supramolecular polymer adhesives: straightforward synthesis and strong substrate interaction. *Angew. Chem. Int. Edit.* **61,** e202203876 (2022).